0026-895X/09/7501-27–34$20.00
MOLECULAR PHARMACOLOGY
Copyright © 2009 The American Society for Pharmacology and Experimental Therapeutics
Mol Pharmacol 75:27–34, 2009

Vol. 75, No. 1
47985/3416206
Printed in U.S.A.

Hydrogen Sulfide Inhibits Rotenone-Induced Apoptosis via Preservation of Mitochondrial Function

Li-Fang Hu, Ming Lu, Zhi-Yuan Wu, Peter T.-H. Wong, and Jin-Song Bian

Department of Pharmacology, Yong Loo Lin School of Medicine, National University of Singapore, Singapore

Received April 15, 2008; accepted October 2, 2008

ABSTRACT

Hydrogen sulfide (H_2S) has been proposed as a novel neuromodulator, which plays critical roles in the central nervous system affecting both neurons and glial cells. However, its relationship with neurodegenerative diseases is unexplored. The present study was undertaken to investigate the effects of H_2S on cell injury induced by rotenone, a commonly used toxin in establishing in vivo and in vitro Parkinson's disease (PD) models, in human-derived dopaminergic neuroblastoma cell line (SH-SY5Y). We report here that sodium hydrosulfide (NaHS), an H_2S donor, concentration-dependently suppressed rotenone-induced cellular injury and apoptotic cell death. NaHS also prevented rotenone-induced p38- and c-Jun NH_2-terminal kinase (JNK)-mitogen-activated protein kinase (MAPK) phosphorylation and rotenone-mediated changes in Bcl-2/Bax levels, mitochondrial membrane potential ($\Delta\Psi_m$) dissipation, cytochrome *c* release, caspase-9/3 activation and poly(ADP-ribose) polymerase cleavage. Furthermore, 5-hydroxydecanoate, a selective blocker of mitochondrial ATP-sensitive potassium (mitoK$_{ATP}$) channel, attenuated the protective effects of NaHS against rotenone-induced cell apoptosis. Thus, we demonstrated for the first time that H_2S inhibited rotenone-induced cell apoptosis via regulation of mitoK$_{ATP}$ channel/ p38- and JNK-MAPK pathway. Our data suggest that H_2S may have potential therapeutic value for neurodegenerative diseases, such as PD.

Although it has been the conventional view that hydrogen sulfide (H_2S) is a noxious gas, there is now accumulating evidence that it is an endogenously produced gaseous messenger and, in particular, serves as an important neuromodulator in the central nervous system (Abe and Kimura, 1996; Kimura, 2002). The production of H_2S in mammalian systems has been attributed to two pyridoxal-5′-phosphate-dependent enzymes: cystathionine β-synthase and cystathionine γ-lyase, both of which use L-cysteine as a substrate (Qu et al., 2008). In human, rat, and bovine brain, cystathionine β-synthase, which is highly expressed in hippocampus and cerebellum, has been identified to be the main enzyme responsible for the biosynthesis of H_2S (Abe and Kimura, 1996). The endogenous level of H_2S in the brain has been reported to be in micromolar concentration range, much higher than that of plasma levels. The cytoprotective and cytotoxic effects of H_2S in various model systems were summarized and reviewed by Szabo (2007).

From a physiological standpoint, H_2S regulates *N*-methyl-D-aspartate receptor-mediated response and thus facilitates the induction of long-term potentiation (Kimura, 2000; Eto et al., 2002b). H_2S also induces calcium waves/elevation in both astrocytes and microglia (Nagai et al., 2004; Lee et al., 2006). From a pathophysiological standpoint, disturbed H_2S synthesis in the brain has been reported in patients with Alzheimer's disease, Down's syndrome, and stroke (Eto et al., 2002a; Qu et al., 2006). We found recently that H_2S attenuates lipopolysaccharide-induced inflammation by inhibiting p38 mitogen-activated protein kinase (MAPK) in microglia (Hu et al., 2007). Kimura and his colleagues have demonstrated that H_2S enhances neuronal activities and protects neurons against oxidative stress via increasing intracellular glutathione levels (Kimura and Kimura, 2004; Umemura and Kimura, 2007). The major intracellular targets of H_2S described in the literature include ATP-sensitive potassium (K_{ATP}) channels and a growing list of intracellular signaling molecules, notably, nuclear factor-κB and p38 MAPK. Among these, the action of H_2S on K_{ATP} channels received more

This work was supported by research grants from Singapore National Medical Research Council (1057/2006) and Singapore Biomedical Research Council (07/1/21/19/509).

Article, publication date, and citation information can be found at http://molpharm.aspetjournals.org.

doi:10.1124/mol.108.047985.

ABBREVIATIONS: MAPK, mitogen-activated protein kinase; 5-HD, 5-hydroxydecanoate; mitoK$_{ATP}$ channel, mitochondrial ATP-sensitive potassium channel; $\Delta\Psi_m$, mitochondrial membrane potential; PD, Parkinson's disease; PARP, poly(ADP-ribose) polymerase; JNK, c-Jun NH_2-terminal kinase; ERK, extracellular signal-regulated kinase; DMSO, dimethyl sulfoxide; MTT, 3-(4,5-dimethylthiazol-2-yl)-2,5-diphenyltetrazolium; PBS, phosphate-buffered saline; PAGE, polyacrylamide gel electrophoresis; TBST, Tris-buffered saline/Tween 20; SB203580, 4-(4-fluorophenyl)-2-(4-methylsulfinylphenyl)-5-(4-pyridyl)1*H*-imidazole; SP600125, anthra(1,9-*cd*)pyrazol-6(2*H*)-one 1,9-pyrazoloanthrone.

attention (Wang, 2002; Yang et al., 2005). We reported recently that H_2S decreases blood pressure in freely moving rats via opening K_{ATP} channels in hypothalamus (Dawe et al., 2008). Thus, H_2S may play important roles in regulating central nervous system functions. Abnormal H_2S production may contribute to the pathogenesis of different brain diseases.

Parkinson's disease (PD) is a neurodegenerative disorder characterized by symptoms including rigidity, resting tremor, and instability of gait and posture. Increasing scientific evidence has demonstrated that microglia-mediated neuroinflammation is critical for the initiation and development of neurodegenerative disorders such as PD. Chemical compounds possessing antineuroinflammatory properties are being considered as promising candidates for PD therapy. Rotenone, which is widely used as a pesticide, has been shown to induce degeneration of dopaminergic neurons in animal models, leading to behavioral and pathological symptoms similar to those of PD (Fleming et al., 2004). To follow up on our previous observation that H_2S produces antineuroinflammatory effects in microglia (Hu et al., 2007), we investigated the effects of H_2S on cell apoptosis/injury in rotenone-treated human-derived dopaminergic neuroblastoma (SH-SY5Y) cells to evaluate whether H_2S may be of potential therapeutic value in the treatment of neurodegenerative diseases, such as PD.

Materials and Methods

Reagents and Antibodies. SB203580 and SP600125 were from Calbiochem (San Diego, CA). All other chemicals used in this study were purchased from Sigma (St. Louis, MO). Antibodies against phospho-JNK (Thr183 and Tyr185), caspase-3, phospho- and total ERK1/2, Bax, and Bcl-2 were purchased from Cell Signaling Technologies (Danvers, MA). Antibodies for detecting cytochrome *c*, total and phospho-p38 (Thr180 and Tyr182), and total JNK1 were obtained from Santa Cruz (Santa Cruz Biotechnology Inc., Santa Cruz, CA).

Rotenone solution in dimethyl sulfoxide (DMSO) was freshly prepared before each treatment. Final DMSO concentration in media did not exceed 0.05%. Because rotenone is lipophilic and may bind to proteins present in the serum, cells were transferred into lower-serum media (0.5% fetal bovine serum) before rotenone treatment to prevent excessive retention of rotenone in the serum.

NaHS was used as an H_2S donor. When NaHS is dissolved in water, HS^- is released and forms H_2S with H^+. This provides a solution of H_2S at a concentration that is approximately 33% of the original concentration of NaHS (Reiffenstein et al., 1992). A recent study reported that sulfide is rapidly removed from the plasma in vivo but remains in both Krebs' and HEPES buffer in vitro in a recirculated system (Whitfield et al., 2008). Therefore, we also examined the concentration of sulfide over time after NaHS (100 μM) was added into Krebs' culture solution (115 mM NaCl, 2.5 mM KCl, 2.46 mM $MgSO_4$, 2 mM $CaCl_2$, 5.6 mM glucose, 1.38 mM NaH_2PO_4, and 25 mM $NaHCO_3$, pH 7.4) for SH-SY5Y cells. We found that sulfide decayed very fast to an undetectable level after incubation in a Petri dish for 30 min in the CO_2 incubator (Fig. 1).

Cell Culture and Treatment. SH-SY5Y cells from the American Type Culture Collection (Manassas, VA) were cultured in Dulbecco's modified Eagle's medium (Invitrogen, Carlsbad, CA) supplemented with 10% (v/v) fetal bovine serum, 0.05 U/ml penicillin, and 0.05 mg/ml streptomycin and maintained at 37°C with 95% humidified air and 5% CO_2.

Cells were usually seeded into 60-mm diameter dishes (except for cytochrome *c* release assay) and incubated overnight. For MAPK (i.e., p38 and JNK) Western blot analysis, regular culture medium was replaced with low-serum media 2 h before rotenone treatment to minimize background kinase activity. For other experiments, regular medium was changed immediately before treatment. Treatment groups include the following: 1) control, cells were treated with vehicle (DMSO); 2) rotenone group, cells were treated with 100 nM rotenone alone for 24 h; 3) H_2S + rotenone group, cells were pretreated with NaHS at indicated concentrations for 30 min before rotenone treatment for further 24 h; and 4) 5-HD + H_2S + rotenone group, 5-HD (200 μM) was added into cell culture 15 min before NaHS application, followed by rotenone treatment.

Total Sulfide Measurement. The procedures are essentially described in the literature with modifications (Gilboa-Garber, 1971). In brief, aliquots (500 μl) of culture solution (Krebs' buffer) were mixed with trichloroacetic acid [10% (w/v), 250 μl], zinc acetate [1% (w/v), 250 μl], *N,N*-dimethyl-*p*-phenylenediamine sulfate (20 μM, 133 μl) in 7.2 M HCl and $FeCl_3$ (30 μM, 133 μl) in 1.2 M HCl in parafilm-enveloped Eppendorf tubes. After 15 min, this mixture was centrifuged at 4000*g* for 10 min. The supernatant was collected, and its absorbance was measured in 96-well plates at a wavelength of 670 nm. All samples were assayed in duplicate and calculated against a calibration curve of NaHS dissolved in Krebs' buffer: 115 mM NaCl, 2.5 mM KCl, 2.46 mM $MgSO_4$, 2 mM $CaCl_2$, 5.6 mM glucose, 1.38 mM NaH_2PO_4, and 25 mM $NaHCO_3$, pH 7.4 .

Cell Viability Assay. Cell viability was evaluated with the MTT method as described previously with modifications (Hu et al., 2005). In brief, the medium was changed before the assay. MTT dissolved in PBS, pH 7.4, was added to the culture media to reach a final concentration of 0.5 mg/ml. After incubation at 37°C for 4 h, the culture media containing MTT were removed. DMSO was then added into each well, and the absorbance at 570 nm was measured.

Quantification of Apoptosis. To visualize nuclear morphology, cells were fixed in 4% paraformaldehyde and stained with 2.5 μg/ml DNA dye Hoechst 33342. Uniformly stained nuclei were scored as healthy, viable cells. Condensed or fragmented nuclei were scored as apoptotic. To obtain unbiased counting, Petri dishes were coded, and cells were scored blindly without knowledge of their prior treatment.

Assessment of Mitochondrial Membrane Potential Loss. Mitochondrial membrane potential ($\Delta\Psi_m$) was detected with fluorescent probe JC-1 (Sigma), which exists predominantly in monomeric form in cells with depolarized mitochondria and displays fluoresced green at 490 nm. Cells with polarized mitochondria predominantly contain JC-1 in aggregate form and show fluorescence of reddish-orange color. Loading was done by incubating SH-SY5Y cells with 2 μM JC-1 for 15 min, rinsed twice with PBS, and visualized by a lab-graded Nikon Optical TE2000-S inverted fluorescence micro-

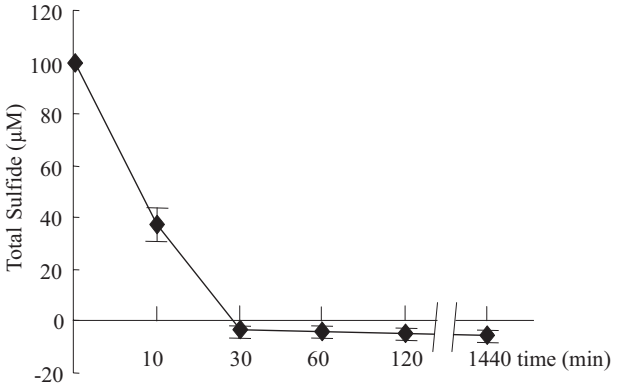

Fig. 1. Colorimetric assay of exogenous sulfide (NaHS) consumption in culture solution (Krebs' buffer) of SH-SY5Y cells. Total NaHS (100 μM) was initially added into sterile Krebs' buffer for cell culture. The total sulfide levels in culture supernatant at different time points were determined with colorimetric assay. Results show a representative time course of sulfide concentrations of three independent measurements.

scope with excitation at 488 nm and emission at >520 nm (Nikon, Tokyo, Japan). Six photos were randomly taken from each well. Fluorescence intensity of the red/green ratio was semiquantitatively determined using ImageJ software (http://rsbweb.nih.gov/ij/). A decrease in this ratio was interpreted as loss of $\Delta\Psi_m$, whereas an increase in the ratio was interpreted as gain in $\Delta\Psi_m$.

Western Blot Analysis. Cells were washed twice with chilled PBS and solubilized in radioimmunoprecipitation assay lysis buffer (Cell Signaling). Protein concentrations were determined by the method of Lowry et al. (1951). Protein samples were separated by 12 to 15% SDS-PAGE and transferred on to a nitrocellulose membrane (GE Healthcare, Chalfont St. Giles, Buckinghamshire, UK). After blocking at room temperature in 10% milk in TBST buffer (10 mM Tris-HCl, 120 mM NaCl, and 0.1% Tween 20, pH 7.4) for 1 h, the membrane was incubated with various primary antibodies at 4°C overnight. Membranes were then washed three times in TBST buffer, followed by incubation with 1:10,000 dilutions of horseradish peroxidase-conjugated anti-rabbit IgG at room temperature for 1 h and washed three times in TBST. Visualization was carried out using an enhanced chemiluminescence kit (GE Healthcare). The density of the bands on Western blots was quantified by densitometry analysis of the scanned blots using ImageQuant software. The relative phosphorylation was normalized to total protein.

Analysis of Cytosolic Cytochrome *c* Accumulation. Cells were seeded in 10-cm diameter dishes at 8×10^5 cells/dish and incubated overnight. Cytochrome *c* release from mitochondria into the cytosol was measured by Western blot analysis. In brief, cells were washed twice with chilled PBS and added with 400 μl of lysis buffer containing 250 mM sucrose, 20 mM HEPES-KOH, pH 7.4, 10 mM KCl, 1.5 mM Na-EGTA, 1.5 mM Na-EDTA, 1 mM $MgCl_2$, 1 mM dithiothreitol, and a cocktail of protease inhibitors (Roche Diagnostics, Indianapolis, IN). After incubation on ice for 5 min, the cells were gently scraped off and centrifuged at 1000*g* for 10 min at 4°C. The supernatants were further centrifuged at 16,000*g* for 25 min at 4°C. The supernatant was collected as cytosolic fraction and subjected to Western blot analysis as mentioned above.

Caspase-9 Activity Assay. Cells were lysed with chilled lysis buffer followed by centrifugation for 1 min at 10,000*g*, and the supernatant (cytosolic extract) was determined with a commercial caspase-9 assay kit according to the manufacturer's instructions (BioVision, Mountain View, CA). The fold increase in activity was calculated as the ratio between values obtained from treated samples versus those obtained in untreated controls.

Statistical Analysis. All data are presented as mean ± S.E.M. Statistical significance was assessed with one-way analysis of variance followed by a post hoc (Bonferroni) test for multiple group comparison. Differences with p value less than 0.05 were considered statistically significant.

Results

H_2S Suppresses Rotenone-Induced Cytotoxicity and Apoptosis. To determine the effect of H_2S on the proapoptotic activity of rotenone, SH-SY5Y cells were treated with rotenone (100 nM for 24 h) in the absence or presence of NaHS, a donor of H_2S. As shown in Fig. 2, rotenone substantially decreased cell viability by 43% compared with that of control. The effect of rotenone was attenuated by NaHS at concentrations from 1 to 300 μM, indicating that H_2S produced protective effects against rotenone-induced cell injury. Treatment with NaHS alone (up to 300 μM) did not show any effect on cell viability (data not shown).

The beneficial effects of H_2S against rotenone-induced apoptosis were further examined by Hoechst 33342 staining assay. Representative photomicrographs of nuclei morphology of SH-SY5Y cells are shown in Fig. 3, a to c. Treatment with rotenone induced condensed and fragmented nuclei, a characteristic of apoptosis. NaHS at 100 μM significantly attenuated this effect (Fig. 3c). Figure 3d shows that NaHS (1–300 μM) concentration-dependently attenuated the proapoptotic activity of rotenone (IC_{50} = approximately 55 μM). This confirms the protective effects of NaHS against rotenone-induced apoptosis in SH-SY5Y cells.

H_2S Prevents Rotenone-Induced $\Delta\Psi_m$ Loss and Inhibits Cytochrome *c* Release. To investigate the mechanisms for the protective effects of NaHS on rotenone-induced apoptosis, $\Delta\Psi_m$ was determined with molecular probe JC-1. As shown in Fig. 4a and quantified in Fig. 4b, as a result of rotenone treatment for 9 h, cells displayed a loss or collapse of $\Delta\Psi_m$, indicated by a shift from red-orange to greenish yellow fluorescence. Pretreatment with NaHS (100 μM) significantly prevented the loss of $\Delta\Psi_m$ in the cells. These findings suggest that cytoprotection by H_2S may be mediated by raising cellular resistance against the initiating steps of apoptosis, namely the decrease of $\Delta\Psi_m$. In addition, Western blot analysis revealed that significant amounts of cytochrome *c* were released from mitochondria into the cytosol in rotenone-treated cells. NaHS (100 μM), which itself had no significant effect, attenuated the stimulatory effect of rotenone on cytochrome *c* release (Fig. 4c). These findings indicate that NaHS may produce antiapoptotic effects via the preservation of mitochondrial function.

H_2S Reverses Rotenone-Induced Changes of Bax and Bcl-2 Levels in SH-SY5Y Cells. Bcl-2, an antiapoptotic protein, prevents the release of cytochrome *c* from mitochondria, whereas Bax, a proapoptotic protein, promotes its release. During apoptosis, Bax translocates to the outer mitochondria membrane to induce mitochondrial membrane permeabilization. This process is blocked by Bcl-2 protein. Therefore, the effects of NaHS on the protein levels of Bcl-2 and Bax were also examined. Rotenone-induced changes of protein levels of Bcl-2 and Bax in the presence and absence of NaHS (Fig. 5). Densitometric analysis indicates that rotenone significantly decreased the basal level of Bcl-2 but increased the Bax protein expression (Fig. 5a). The ratio of Bcl-2 over Bax was decreased by 40% in rotenone-treated

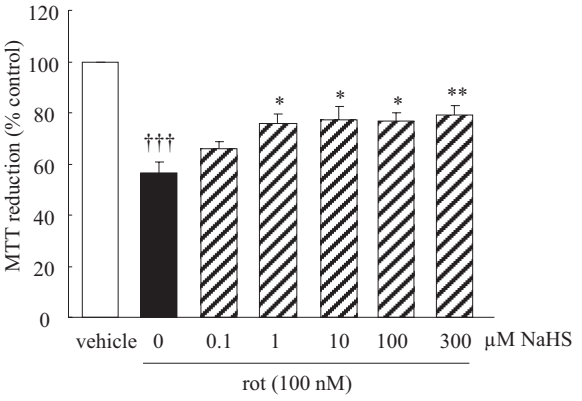

Fig. 2. Effects of NaHS on rotenone-induced cytotoxicity in SH-SY5Y cells. Cell viability was determined using MTT method. Values are expressed as the percentage of the untreated control and represented as mean ± S.E.M. of at least five independent experiments. †††, $p < 0.001$ versus control; *, $p < 0.05$; **, $p < 0.01$ versus rotenone group, respectively.

cells (Fig. 5b). This effect was markedly attenuated by NaHS (100 μM).

H_2S Decreases Rotenone-Induced Caspase-9/3 Activation and Poly(ADP-ribose) Polymerase Cleavage. The cytochrome *c*, together with Apaf-1 and pro-caspase-9, may form apoptosome, which activates caspase-9 and its downstream caspase cascades. It was found that rotenone increased the caspase-9 activity by 2.5-fold compared with that of the control group. This increase was attenuated by NaHS (100 μM) (Fig. 6a). Caspase-3 is a critical executioner of apoptosis, and the pro-caspase-3 can be cleaved by active caspase-9. As shown in Fig. 6b, treatment of the cells with rotenone significantly induced the cleavage of pro-caspase-3 (35 kDa) to its 19- and 17-kDa subunits, which was dramatically inhibited by NaHS (100 μM). Our data suggest that rotenone did activate caspase-3 in SH-SY5Y cells and that this activation could be suppressed by NaHS.

Poly(ADP-ribose) polymerase (PARP) is an enzyme implicated in DNA damage and repair mechanisms. Cleavage of PARP by active caspase-3 from native 116 to 89 kDa is a hallmark of apoptosis. We then examined the effect of H_2S on rotenone-induced apoptosis in SH-SY5Y cells by measuring PARP cleavage using Western blot analysis. As shown in Fig. 6c, treatment with rotenone increased the cleavage of PARP by 3.8-fold in SH-SY5Y cells. Pretreatment with NaHS (10–300 μM) for 30 min significantly reduced PARP cleavage induced by rotenone in a concentration-dependent manner (Fig. 6c).

The Protective Effects of H_2S Involves mitoK$_{ATP}$ Channels. To examine the involvement of mitoK$_{ATP}$ channels, 5-HD (200 μM), a selective mitoK$_{ATP}$ channel blocker, was given 15 min before NaHS application. It is interesting that 5-HD, which had no effect by itself, significantly attenuated the inhibitory effects of NaHS on rotenone-induced cytochrome *c* release, caspase-9 activity, cell injury, and PARP cleavage (Fig. 7, a–d). These data suggest that the initial exposure to NaHS resulted in the opening of mitoK$_{ATP}$ channels located in inner mitochondrial membrane, which in turn mediate the subsequent signaling cascade leading to the observed neuroprotective effects.

Rotenone Induces p38/JNK MAPK Activation. Both p38 and JNK signaling pathways are critical for the degeneration of dopaminergic neuronal cells (Newhouse et al., 2004). We therefore further studied the contribution of MAPK to the neuroprotective effects of H_2S. It was found that phosphorylation of p38 MAPK occurred as early as 5 min and reached the peak at 15 min after rotenone treatment. This effect gradually reduced and disappeared by 4 h after treatment (Fig. 8a). Rotenone also induced the phosphorylation of JNK but with a slower time course. The peak effect occurred at 4 h and almost disappeared by 24 h after treatment (Fig. 8b).

In addition, SB203580 (a p38 MAPK inhibitor) and SP600125 (a selective JNK inhibitor) markedly attenuated rotenone-in-

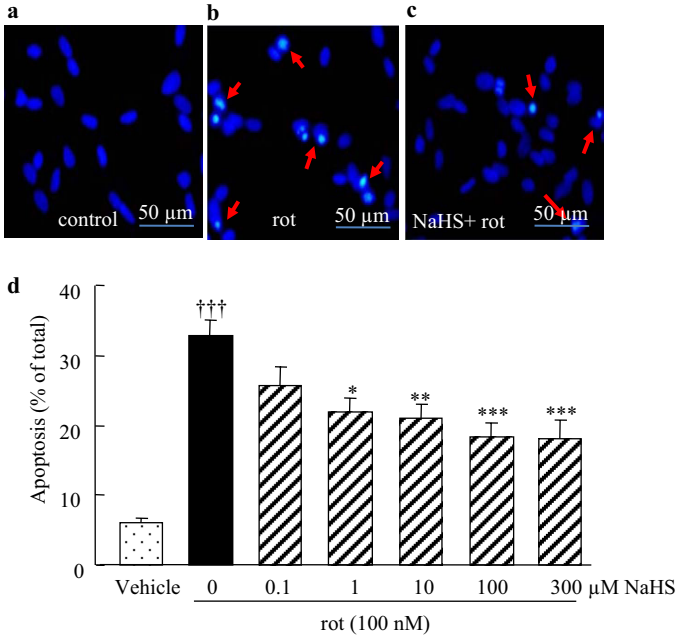

Fig. 3. Effects of NaHS on rotenone-induced cell apoptosis in SH-SY5Y cells. Cell apoptosis was detected by Hoechst 33342 staining in cells treated with vehicle (a), rotenone (b, 100 nM, rot), and NaHS (c, 100 μM) + rot. Arrows identify cells with condensed or fragmented nuclei, characteristic of apoptosis. d, quantification of apoptosis based on nuclear condensation or fragmentation. Data were expressed as mean ± S.E.M. for at least seven independent experiments. †††, $p < 0.001$ versus control; *, $p < 0.05$; **, $p < 0.01$; ***, $p < 0.001$ versus rotenone group, respectively.

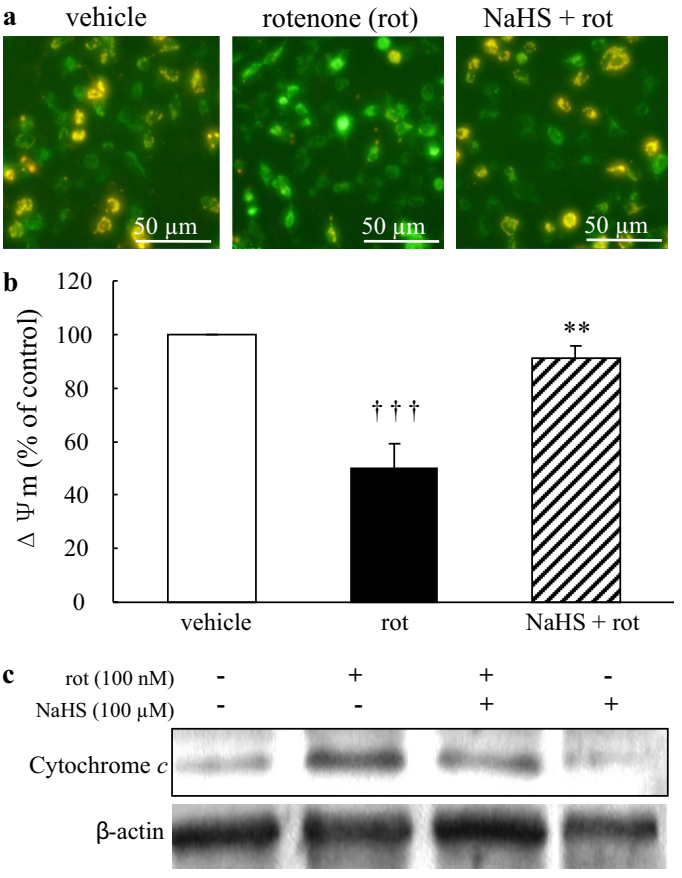

Fig. 4. Effects of NaHS on rotenone-induced $\Delta\Psi_m$ loss and cytochrome c release in SH-SY5Y cells. a, representative cells stained with JC-1 from different groups. b, bar chart shows the quantified data of four independent experiments. Quantification of $\Delta\Psi_m$ expressed as the ratio of J-aggregate to JC-1 monomer (red/green) fluorescence intensity. Data are expressed as mean ± S.E.M. c, representative immunoblots for cytochrome *c* release from three independent experiments. Cytosolic fractions of the extract were subjected to 15% SDS-PAGE and immunoblotted with anti-cytochrome *c* antibody. β-Actin was used as a control for equal loading. †††, $p < 0.001$ versus control; **, $p < 0.01$ versus rotenone group.

duced cell injury (Fig. 8c) and apoptosis (Fig. 8d) in SH-SY5Y cells. These data further confirmed that both p38 and JNK MAPK are involved in the mediation of the effects of rotenone.

H_2S Attenuates Rotenone-Induced p38/JNK MAPK Activation. To study the signaling mechanisms of the neuroprotective effects of H_2S, we also studied the concentration-dependent effects of H_2S on rotenone-induced stimulation of p38/JNK MAPK. As shown in Fig. 9, the maximal effects of rotenone on the phosphorylation of both p38 (at 15 min, Fig. 9a) and JNK (at 4 h, Fig. 9b) were attenuated by NaHS (1–300 μM) in a concentration-dependent manner. These data strongly suggest that the antiapoptotic effects of NaHS are associated with inhibition of the p38/JNK signaling pathways.

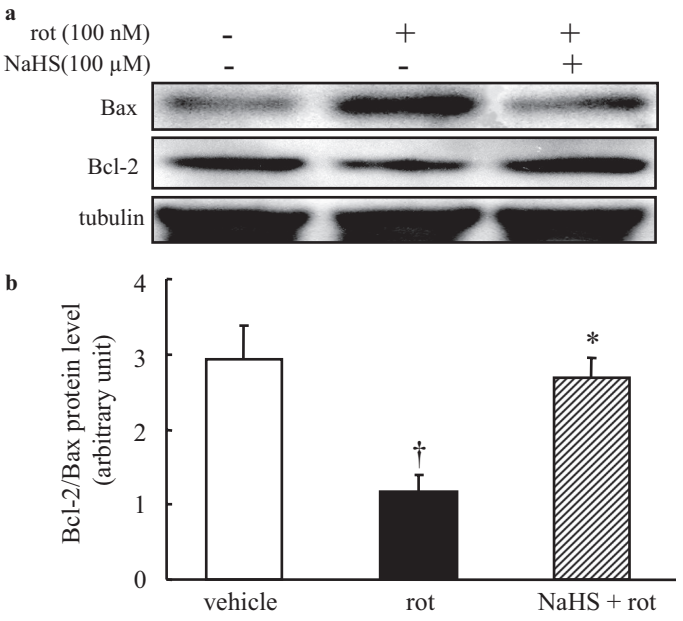

Fig. 5. Effects of NaHS on rotenone-induced alterations of Bcl-2 and Bax level in SH-SY5Y cells. Total protein extracts were subjected to 15% SDS-PAGE for Western blot analysis. a, representative images from four different experiments. Tubulin was used as a loading control. b, densitometric analysis performed by normalizing Bcl-2 proteins to Bax proteins signals. Data were expressed as the mean ± S.E.M. †, $p < 0.05$ versus control; *, $p < 0.05$ versus rotenone group.

Discussion

Rotenone is a naturally occurring toxin and a commonly used pesticide to reproduce the neurochemical, neuropathological, and behavioral features of PD in rats. In the present study, we demonstrated for the first time that NaHS was able to inhibit rotenone-mediated cytotoxicity and apoptosis in a concentration-dependent manner. The underlying mechanisms may be associated with suppression of rotenone-induced events, including $\Delta\Psi_m$ loss, release of cytochrome *c*, and activation of subsequent caspase cascades via regulation of mitoK_{ATP} channels/ p38- and JNK-MAPK pathway (Fig. 10).

Mitochondrial dysfunction is a prominent feature in apoptosis (Lemasters et al., 2002). Rotenone is a complex I inhibitor. The inhibition of complex I may induce $\Delta\Psi_m$ loss and the release of proapoptotic proteins (e.g., cytochrome *c*) from the mitochondrial intermembrane space to cytosol, where cytochrome *c* forms oligomeric complex with Apaf-1 and activates caspase-9. Our data showed that H_2S prevented rotenone-induced $\Delta\Psi_m$ loss and cytosolic accumulation of cytochrome *c*, suggesting that H_2S may produce neuroprotective effects via the preservation of mitochondrial function. The increased mitochondrial permeabilization and release of cytochrome *c* may also be regulated by proapoptotic proteins, such as Bax. In apoptotic cells, Bax interacts with Bid, and the resultant conformational change causes Bax to translocate from cytoplasm to the mitochondria, where it promotes the opening of permeability transition pore and thereby mediates the efflux of cytochrome *c*. This process could be blocked by mitochondrial protein Bcl-2. Hence, the ratio of Bcl-2/Bax may be used to indicate mitochondrial permeability. Consistent with previous findings (De Sarno et al., 2003), we found that rotenone decreased the ratio of Bcl-2/Bax protein in SH-SY5Y cells. This effect was significantly attenuated by H_2S. Thus, the protective effects of H_2S on mitochondrial function may also occur via suppression of the expression of the proapoptotic proteins.

The release of cytochrome *c* and apoptosis-inducing factor from mitochondria to cytosol may further stimulate caspase-9, which may lead to the activation of caspase-3 and subsequent degradation of cellular death substrates (e.g., PARP). We found in the present study that NaHS attenuated the effects of rote-

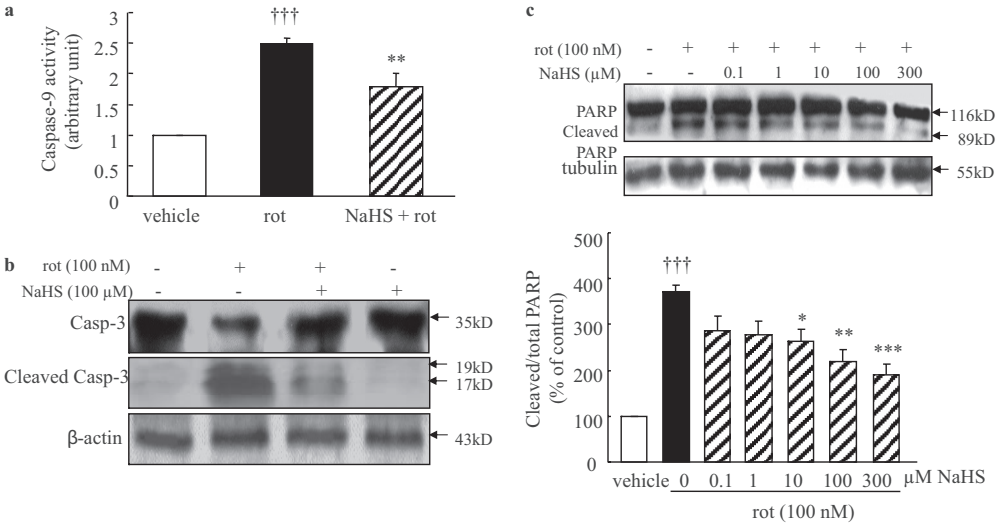

Fig. 6. Effects of NaHS on rotenone-induced caspase-3/9 activation and PARP cleavage in SH-SY5Y cells. a, mean data showing NaHS attenuated rotenone (rot) induced caspase-9 activation. Results are normalized by the control values. b and c, the levels of cleaved caspase-3 (b) and PARP (c) were determined by Western blot. Data were expressed by the ratio of cleaved PARP over total (uncleaved plus cleaved) PARP. Tubulin and β-actin were used as controls for equal loading. Mean ± S.E.M.; $n = 4$ to 8 independent experiments. †††, $p < 0.001$ versus control; *, $p < 0.05$; **, $p < 0.01$; ***, $p < 0.001$ versus rotenone group, respectively.

none on caspase-9/3 activation and PARP degradation and therefore protected cells against apoptotic injury. The effects of NaHS on this signaling cascade may be derived from the preservation of mitochondrial function via prevention of $\Delta\Psi_m$ loss and inhibition of cytochrome *c* release.

Similar to the findings by Whitfield et al. (2008), we found that H_2S concentration decayed rapidly (within 30 min) in the culture solution. Therefore, it seemed that H_2S level was reaching undetectable levels before the addition of rotenone in our present experimental setting. Therefore, the obvious question is how H_2S may protect cells against rotenone-induced injury. Recent studies have suggested that H_2S plays a critical role in opening K_{ATP} channels (Wang, 2002; Yang et al., 2005; Dawe et al., 2008), which contributes to neuroprotective effects (Busija et al., 2004; Wu et al., 2006). The role of K_{ATP} channels in PD has been addressed as well. Activation of mitoK_{ATP} channel protects against rotenone-induced cell death and neurochemical alterations in rats (Tai et al., 2003; Zhou et al., 2007). By examining the involvement of mitoK_{ATP} channels in the neuroprotective effects of H_2S,

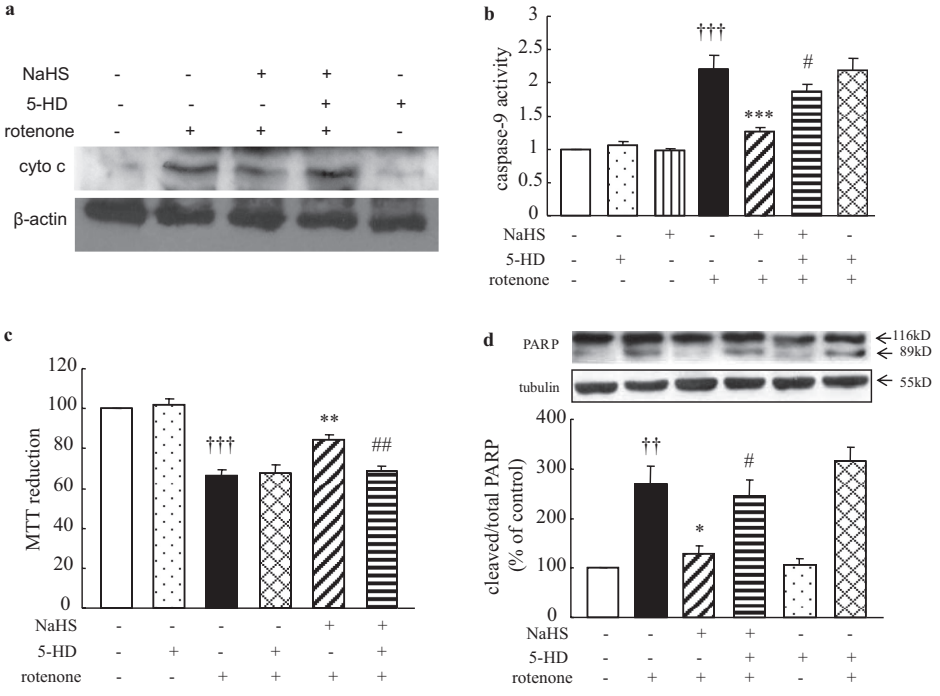

Fig. 7. Effect of mitoK_{ATP} channels blocker 5-HD on the protective effects of NaHS against rotenone-induced cytochrome *c* release (a), caspase-9 activation (b), cell injury (c), and PARP cleavage (d) in SH-SY5Y cells. Cells were pretreated with NaHS for 30 min before rotenone treatment for 24 h. 5-HD (200 μM) was added into cells before NaHS treatment. Data are presented as the percentage of control value and expressed as mean ± S.E.M. ††, $p < 0.01$; †††, $p < 0.001$ versus control; *, $p < 0.05$; **, $p < 0.01$; ***, $p < 0.001$ versus rotenone group; #, $p < 0.05$; ##, $p < 0.01$ versus NaHS + rotenone group.

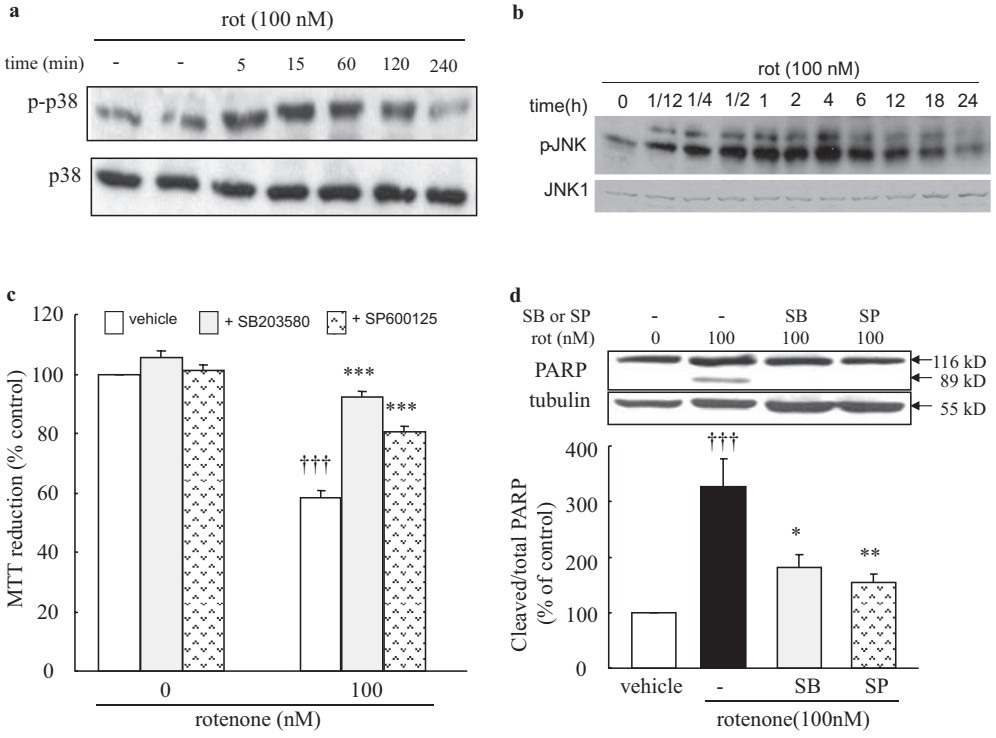

Fig. 8. Rotenone stimulates both p38 and JNK MAPK in SH-SY5Y cells. a and b, time course for the effects of rotenone on phosphorylation of p38 (a) and JNK (b). c and d, blockade of p38 MAPK with SB203580 (10 μM) and JNK with SP600125 (10 μM) attenuated rotenone-induced cell injury assayed by MTT method (c) and PARP cleavage (d). Data are presented as the percentage of control value and expressed as mean ± S.E.M. †††, $p < 0.001$ versus control; *, $p < 0.05$; **, $p < 0.01$; ***, $p < 0.001$ versus rotenone group, respectively.

we found that blockade of mitoK_{ATP} channels with 5-HD attenuated the protective effects of H_2S on rotenone-induced cell apoptosis. These findings suggest that H_2S rapidly opens mitoK_{ATP} channels, which, in turn, trigger a series of persistent intracellular responses, including inhibition of MAPK signaling pathway and preservation of mitochondrial integrity (Zhang et al., 2007). This triggering effect of H_2S may be similar to the mechanism for the cardioprotection conferred by H_2S preconditioning (Pan et al., 2008). It is interesting that it was also reported that H_2S can be rapidly absorbed in a kind of sulfur store in a form of bound sulfane sulfur and then gradually released upon stimulation (Warenycia et al., 1990; Ogasawara et al., 1993). Therefore, this may also explain the persistent protective effects of H_2S despite its short half-life.

Stimulation of MAPK (i.e., ERK1/2, p38, and JNK) leads to a wide range of cellular responses, including growth, differentiation, inflammation, and apoptosis. Because rotenone only stimulates the activities of JNK and p38, but not that of ERK1/2, in SH-SY5Y cells (Newhouse et al., 2004), we therefore only investigated the role of H_2S in rotenone-induced phosphorylation of p38 and JNK in the present study. We found that H_2S concentration-dependently inhibited the activation of these two kinases. The involvement of p38 MAPK in the neuroprotective effects has also been reported by our and other groups. Rinaldi et al. (2006) found that H_2S promotes the survival of the human polymorphonuclear cells via inhibition of p38 and caspase-3 (Rinaldi et al., 2006). We recently reported that H_2S attenuates lipopolysaccharide-stimulated p38 activation in microglial cells (Hu et al., 2007). All of these findings indicate that inhibition of p38 may contribute to the protective effects of H_2S. Because p38 MAPK was shown to mediate proapoptotic protein Bax-induced mitochondrial membrane permeabilization and neuro-

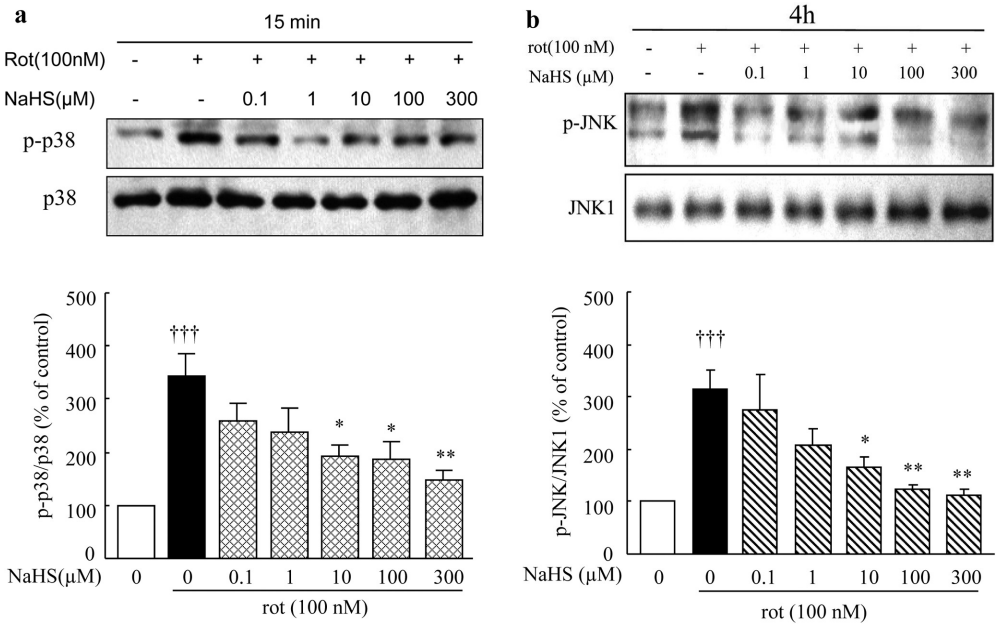

Fig. 9. Concentration-dependent effects of NaHS (0.1–300 μM) on rotenone-induced activation of p38 (a) and JNK (b) MAPK in SH-SY5Y cells. Data are presented as mean ± S.E.M. of 6 independent experiments. †††, $p < 0.001$ versus control; *, $p < 0.05$; **, $p < 0.01$ versus rotenone group, respectively.

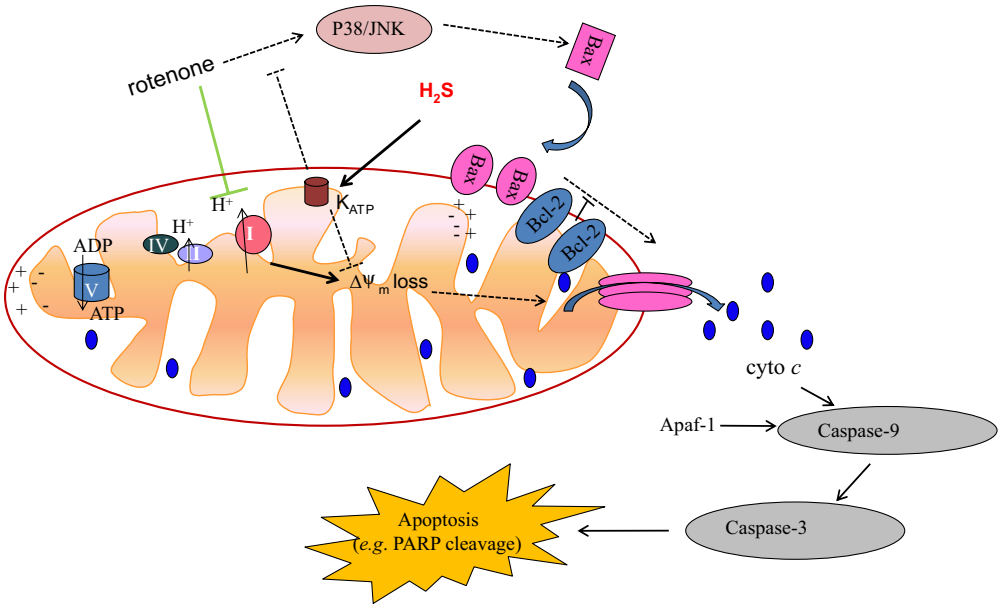

Fig. 10. Proposed signaling mechanisms for the effects of H_2S on rotenone-induced apoptosis. Rotenone induces complex I inhibition, which initiates the dissipation of $\Delta\Psi_m$, causing the matrix swelling and promoting the opening of mitochondrial permeability transition pore. Rotenone may also stimulate intracellular p38/JNK MAPK pathway. The activation of p38/JNK MAPK, in turn, induces the recruitment of cytoplasmic apoptotic members of Bcl-2 family proteins (e.g., Bax, Bid) to mitochondria and forms permeability transition pore, causing the release of cytochrome *c* to cytosol. The cytosolic apoptotic executors (cytochrome *c*, Apaf-1, and pro-caspase-9) form apoptosome, which leads to activation of pro-caspase-9, subsequently activating caspase-3. The mechanisms underlying the antiapoptotic effects of H_2S may result from opening of mitoK_{ATP} channels, which in turn mediates the prevention of $\Delta\Psi_m$ loss and the inhibition of p38/JNK MAPK pathway.

nal apoptosis (Gomez-Lazaro et al., 2007), the antiapoptotic effect of H_2S may be associated with the suppression of the activation of both p38 and JNK MAPK caused by rotenone.

The glutathione (GSH) redox cycle is a major endogenous protective system and an important component of the antioxidant machinery of the nervous system (Seyfried et al., 2000). Recent evidence indicates that depletion of cellular GSH results in the accumulation of ROS and loss of mitochondrial function (Bharat et al., 2002). Rotenone also induces the depletion of intracellular GSH and the accumulation of ROS, which in turn activates p38/JNK MAPK in the cells. It has previously been demonstrated that H_2S protects neuronal cells against oxidative stress via increasing GSH production (Kimura and Kimura, 2004). It is therefore logical to expect that GSH also contributes to the antiapoptotic effects of H_2S on rotenone-treated SH-SY5Y cells, but more experiments are warranted to further confirm this hypothesis.

In conclusion, the present observations identify a beneficial role of H_2S against rotenone-induced apoptosis in SH-SY5Y cells via regulation of mitoK_{ATP} channels and inhibition of p38 and JNK pathway. Because epidemiological studies have revealed a correlation between general pesticide (i.e., rotenone) exposure and increased risk for PD, our findings may therefore provide a potential venue to treat PD.

Acknowledgments

We thank Ester Khin Sandar Win for technical support.

References

Abe K and Kimura H (1996) The possible role of hydrogen sulfide as an endogenous neuromodulator. *J Neurosci* **16:**1066–1071.
Bharat S, Cochran BC, Hsu M, Liu J, Ames BN, and Andersen JK (2002) Pretreatment with R-lipoic acid alleviates the effects of GSH depletion in PC12 cells: implications for Parkinson's disease therapy. *Neurotoxicology* **23:**479–486.
Busija DW, Lacza Z, Rajapakse N, Shimizu K, Kis B, Bari F, Domoki F, and Horiguchi T (2004) Targeting mitochondrial ATP-sensitive potassium channels—a novel approach to neuroprotection. *Brain Res Brain Res Rev* **46:**282–294.
Dawe GS, Han SP, Bian JS, and Moore PK (2008) Hydrogen sulphide in the hypothalamus causes an ATP-sensitive K^+ channel-dependent decrease in blood pressure in freely moving rats. *Neuroscience* **152:**169–177.
De Sarno P, Shestopal SA, King TD, Zmijewska A, Song L, and Jope RS (2003) Muscarinic receptor activation protects cells from apoptotic effects of DNA damage, oxidative stress, and mitochondrial inhibition. *J Biol Chem* **278:**11086–11093.
Eto K, Asada T, Arima K, Makifuchi T, and Kimura H (2002a) Brain hydrogen sulfide is severely decreased in Alzheimer's disease. *Biochem Biophys Res Commun* **293:**1485–1488.
Eto K, Ogasawara M, Umemura K, Nagai Y, and Kimura H (2002b) Hydrogen sulfide is produced in response to neuronal excitation. *J Neurosci* **22:**3386–3391.
Fleming SM, Zhu C, Fernagut PO, Mehta A, DiCarlo CD, Seaman RL, and Chesselet MF (2004) Behavioral and immunohistochemical effects of chronic intravenous and subcutaneous infusions of varying doses of rotenone. *Exp Neurol* **187:**418–429.
Gilboa-Garber N (1971) Direct spectrophotometric determination of inorganic sulfide in biological materials and in other complex mixtures. *Anal Biochem* **43:**129–133.
Gomez-Lazaro M, Galindo MF, Melero-Fernandez de Mera RM, Fernandez-Gómez FJ, Concannon CG, Segura MF, Comella JX, Prehn JH, and Jordan J (2007) Reactive oxygen species and p38 mitogen-activated protein kinase activate Bax to induce mitochondrial cytochrome c release and apoptosis in response to malonate. *Mol Pharmacol* **71:**736–743.
Hu LF, Wang S, Shi XR, Yao HH, Sun YH, Ding JH, Liu SY, and Hu G (2005) ATP-sensitive potassium channel opener iptakalim protected against the cytotoxicity of MPP^+ on SH-SY5Y cells by decreasing extracellular glutamate level. *J Neurochem* **94:**1570–1579.
Hu LF, Wong PT, Moore PK, and Bian JS (2007) Hydrogen sulfide attenuates lipopolysaccharide-induced inflammation by inhibition of p38 mitogen-activated protein kinase in microglia. *J Neurochem* **100:**1121–1128.
Kimura H (2000) Hydrogen sulfide induces cyclic AMP and modulates the NMDA receptor. *Biochem Biophys Res Commun* **267:**129–133.
Kimura H (2002) Hydrogen sulfide as a neuromodulator. *Mol Neurobiol* **26:**13–19.
Kimura Y and Kimura H (2004) Hydrogen sulfide protects neurons from oxidative stress. *FASEB J* **18:**1165–1167.
Lee SW, Hu YS, Hu LF, Lu Q, Dawe GS, Moore PK, Wong PT, and Bian JS (2006) Hydrogen sulphide regulates calcium homeostasis in microglial cells. *Glia* **54:**116–124.
Lemasters JJ, Qian T, He L, Kim JS, Elmore SP, Cascio WE, and Brenner DA (2002) Role of mitochondrial inner membrane permeabilization in necrotic cell death, apoptosis, and autophagy. *Antioxid Redox Signal* **4:**769–781.
Lowry OH, Rosebrough NJ, Farr AL, and Randall RJ (1951) Protein measurement with the folin phenol reagent. *J Biol Chem* **193:**265–275.
Nagai Y, Tsugane M, Oka J, and Kimura H (2004) Hydrogen sulfide induces calcium waves in astrocytes. *FASEB J* **18:**557–559.
Newhouse K, Hsuan SL, Chang SH, Cai B, Wang Y, and Xia Z (2004) Rotenone-induced apoptosis is mediated by p38 and JNK MAP kinases in human dopaminergic SH-SY5Y cells. *Toxicol Sci* **79:**137–146.
Ogasawara Y, Ishii K, Togawa T, and Tanabe S (1993) Determination of bound sulfur in serum by gas dialysis/high-performance liquid chromatography. *Anal Biochem* **215:**73–81.
Pan TT, Neo KL, Hu LF, Yong QC, and Bian JS. (2008) H2S preconditioning-induced PKC activation regulates intracellular calcium handling in rat cardiomyocytes. *Am J Physiol Cell Physiol* **294:**C169–C177.
Qu K, Chen CP, Halliwell B, Moore PK, and Wong PT (2006) Hydrogen sulfide is a mediator of cerebral ischemic damage. *Stroke* **37:**889–893.
Qu K, Lee SW, Bian JS, Low CM, and Wong PT (2008) Hydrogen sulfide: neurochemistry and neurobiology. *Neurochem Int* **52:**155–165.
Reiffenstein RJ, Hulbert WC, and Roth SH (1992) Toxicology of hydrogen sulfide. *Annu Rev Pharmacol Toxicol* **32:**109–134.
Rinaldi L, Gobbi G, Pambianco M, Micheloni C, Mirandola P, and Vitale M (2006) Hydrogen sulfide prevents apoptosis of human PMN via inhibition of p38 and caspase 3. *Lab Investig* **86:**391–397.
Seyfried J, Soldner F, Kunz WS, Schulz JB, Klockgether T, Kovar KA, and Wüllner U (2000) Effect of 1-methyl-4-phenylpyridinium on glutathione in rat pheochromocytoma PC 12 cells. *Neurochem Int* **36:**489–497.
Szabó C (2007) Hydrogen sulphide and its therapeutic potential. *Nat Rev Drug Discov* **6:**917–935.
Tai KK, McCrossan ZA, and Abbott GW (2003) Activation of mitochondrial ATP-sensitive potassium channels increases cell viability against rotenone-induced cell death. *J Neurochem* **8:**1193–1200.
Umemura K and Kimura H (2007) Hydrogen sulfide enhances reducing activity in neurons: neurotrophic role of H2S in the brain? *Antioxid Redox Signal* **9:**2035–2041.
Wang R (2002) Two's company, three's a crowd: can H2S be the third endogenous gaseous transmitter? *FASEB J* **16:**1792–1798.
Warenycia MW, Goodwin LR, Francom DM, Dieken FP, Kombian SB, and Reiffenstein RJ (1990) Dithiothreitol liberates non-acid labile sulfide from brain tissue of H2S-poisoned animals. *Arch Toxicol* **64:**650–655.
Whitfield NL, Kreimier EL, Verdial FC, Skovgaard N, and Olson KR (2008) Reappraisal of H2S/sulfide concentration in vertebrate blood and its potential significance in ischemic preconditioning and vascular signaling. *Am J Physiol Regul Integr Comp Physiol* **294:**R1930–R1937.
Wu L, Shen F, Lin L, Zhang X, Bruce IC, and Xia Q (2006) The neuroprotection conferred by activating the mitochondrial ATP-sensitive K^+ channel is mediated by inhibiting the mitochondrial permeability transition pore. *Neurosci Lett* **402:**184–189.
Yang W, Yang G, Jia X, Wu L, and Wang R (2005) Activation of KATP channels by H2S in rat insulin-secreting cells and the underlying mechanisms. *J Physiol* **569:**519–531.
Zhang S, Zhou F, Ding JH, Zhou XQ, Sun XL, and Hu G (2007) ATP-sensitive potassium channel opener iptakalim protects against MPP-induced astrocytic apoptosis via mitochondria and mitogen-activated protein kinase signal pathways. *J Neurochem* **103:**569–579.
Zhou F, Wu JY, Sun XL, Yao HH, Ding JH, and Hu G (2007) Iptakalim alleviates rotenone-induced degeneration of dopaminergic neurons through inhibiting microglia-mediated neuroinflammation. *Neuropsychopharmacology* **32:**2570–2580.

Address correspondence to: Dr. Jin-Song Bian, Department of Pharmacology, Yong Loo Lin School of Medicine, National University of Singapore, Singapore, 117597. E-mail: phcbjs@nus.edu.sg.

MOL PHARM

Correction to "Hydrogen Sulfide Inhibits Rotenone-Induced Apoptosis via Preservation of Mitochondrial Function"

In the above article [Hu LF, Lu M, Wu ZY, Wong PTH, and Bian JS (2009) *Mol Pharmacol* **75:**27–34], Fig. 7a, Fig. 8b, and the top panel of Fig. 9a are incorrect. The corrected figures are shown below.

The online version of this article has been corrected in departure from the print version.

The authors regret this error and apologize for any confusion or inconvenience it may have caused.

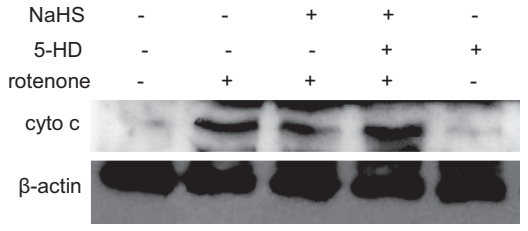

Fig. 7a.

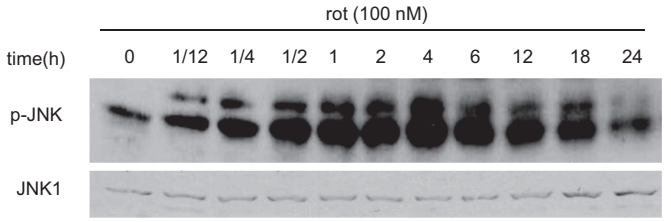

Fig. 8b.

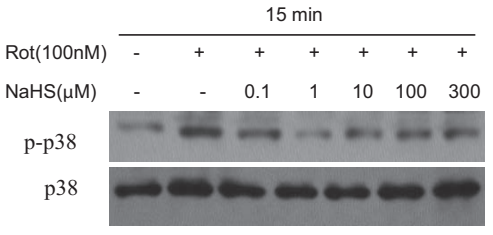

Fig. 9a. Top panel.